

2 kW Pulse Power from Internal Wavelength Stabilized Diode Laser Bar for LiDAR Applications

A. Knigge*, N. Ammouri, H. Christopher, J. Glaab, A. Liero, J. Fricke, H. Wenzel

Ferdinand-Braun-Institut (FBH), 12489 Berlin, Germany

*Email: andrea.knigge@fbh-berlin.de

Abstract –We present a bipolar-cascade distributed-Bragg-reflector laser bar with an intended wavelength of 905 nm emitting 8 ns long pulses with 2 kW peak power at a current slightly above 1 kA into the third vertical mode. The spectral width of the pulses is 0.3 nm.

I. Introduction

Lasers generating short (ns range) optical pulses are key components for Light Detection and Ranging (LiDAR) systems used for, e.g., autonomous driving or the measurements of atmospheric parameters. Although semiconductor lasers are ideally suited for generation of ns pulses simply by turning the injection current on and off, the available optical peak powers or pulse energies are either too low [1] or the needed current amplitudes are too high [2].

In order to reduce the currents needed to achieve high peak powers, several laser diodes, separated by tunnel junctions can be epitaxially stacked in series [3-7]. Ideally, the slope efficiencies of such nanostack lasers are proportional to the number N of diodes. Thus, far above threshold, the optical power is increased by a factor of N compared to single diodes for the same injection current, at the expense of a correspondingly increased voltage. Recently, we reported the successful stacking of three active regions alternating with tunnel junctions in a single waveguide core instead of stacking independently working laser diodes [8]. In order to minimize the impact of the large absorption resulting from the highly doped tunnel junctions and to maximize the modal gain, we designed the waveguide in such a way that the tunnel junctions and active regions are placed into the nodes and antinodes, respectively, of the intensity for the third vertical mode. We obtained a total slope efficiency of 3.6 W/A for as-cleaved 1 mm long broad area Fabry-Pérot (FP) lasers emitting near 905 nm. This concept of a shared waveguide mode enabled the implementation of a surface Bragg grating for wavelength stabilization [9], which is needed to improve the signal-to-noise ratio in LiDAR systems. Based on these results, we realized a distributed Bragg reflector (DBR) laser bar consisting of 48 emitters and integrated it into an electrical driver circuit developed in-house delivering ns current pulses with amplitudes of more than 1 kA. In this summary, we present results of an electro-optical characterization.

II. Results

The vertical layer structure consists of GaAs buffer, $\text{Al}_{0.5}\text{Ga}_{0.5}\text{As}$ n-cladding, $\text{Al}_{0.45}\text{Ga}_{0.55}\text{As}$ optical confinement layers around the active regions and tunnel junctions, $\text{Al}_{0.75}\text{Ga}_{0.25}\text{As}$ p-cladding, and GaAs cap. The three 6 nm thick InGaAs active quantum wells (QWs) and the two 35 nm thick GaAs tunnel junctions (TJs) were placed into the antinodes and nodes, respectively, of the third vertical mode (Fig. 1). The total thickness of the waveguide core including active regions and tunnel junctions is about 5.5 μm .

The 1 cm wide DBR laser bar was fabricated in a standard wafer process. It consists of 48 single emitters with a stripe width of the p-contact of 50 μm and a total cavity length of 4 mm. Narrow trenches shallowly etched into the epitaxial layers provide lateral optical as well as current confinement. Electrical isolation is achieved by the deposition of an insulator layer opened on top of the etched mesa. 1 mm long Bragg gratings stabilizing the wavelength were defined by e-beam lithography on parts of the surface of the completely grown wafer and transferred into the semiconductor by plasma etching [10]. The grating period of 970.7 nm corresponding to a 7th Bragg order was chosen to allow for an intended Bragg wavelength of 905 nm. A scanning electron microscope (SEM) picture of a grating etched into a process control area on the wafer is shown in Fig. 1. After processing, the facets of cleaved bars were coated to achieve reflection coefficients of 1% (gain section) and nearly 0% (Bragg section). The laser bar was soldered p-side down on a CuW submount and integrated into an electrical driver developed in-house. The driver generates electrical pulses with pulse lengths between 5 and 15 ns. To obtain the desired peak currents of up to 1 kA, four driver units were combined into a single module.

The pulse power in dependence on the pulse current of the 48-emitter bar mounted into the quadrupole driver module is shown in Fig. 2. An optical pulse power of more than 2 kW is reached at a pulse current slightly above 1 kA for both temperatures of 25°C and 45°C. Both the pulse power and the pulse current were calculated from the time-averaged values measured assuming widths of the optical and electrical pulses of 8 ns and a repetition frequency of 10 kHz. The threshold current is about 0.08 kA and the slope efficiency 2.3 W/A up to a power of 0.5 kW. The efficiency is more than twice as large as that of a similar laser having only a single active region.

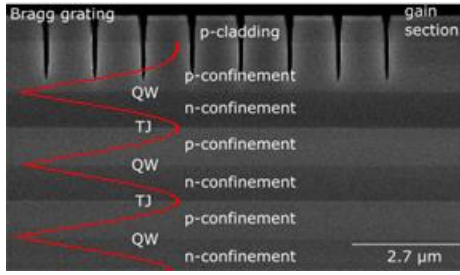


Fig. 1. Cross-sectional SEM picture along the cavity axis of a DBR laser showing parts of the Bragg grating (left) and the gain section (right) and superimposed mode profile (red).

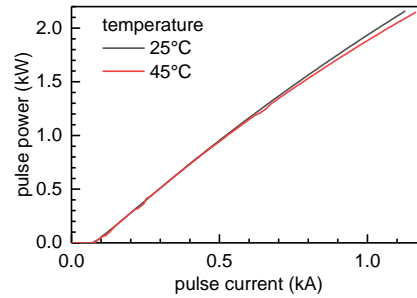


Fig. 2. Optical output power emitted at the front facet of the DBR laser bar versus the injection current at temperatures of 25°C (black) and 45°C (red) for a pulse width of 8 ns.

The optical spectra have a full-width at half maximum (FWHM) of about 0.3 nm for both temperatures, see Fig. 3. The temperature-dependent shift of the peak wavelength is determined to be about 0.07 nm/K which is much smaller than the corresponding shift of the gain peak governing the lasing wavelength of a FP laser (0.3–0.4 nm/K in the 9xx nm wavelength range). The side peak originates from an additional peak of the reflection spectrum with an offset of ~ 2 nm from the main reflection peak towards shorter wavelengths [9] and the location of the gain peak at an even shorter wavelength. With increasing temperature, the side peaks move with the same rate as the main peak, but their intensity decreases because of the stronger shift of the gain peak wavelength.

The temporal behaviour of the optical pulse measured with a fast photodiode and an oscilloscope is exemplarily shown in Fig. 4 for a pulse current of 0.79 kA. The rise time of the optical power from turn-on up to the peak value is about 10 ns. The power drops quickly to 20% of the peak value within 5 ns, followed by a slower decay. The FWHM of the pulse is 8 ns, in agreement with the value assumed in Fig. 2.

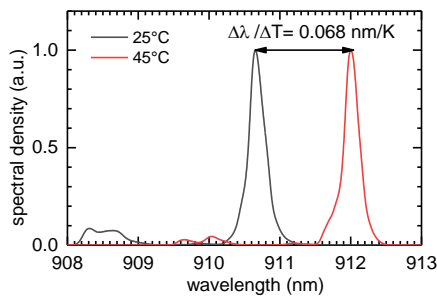


Fig. 3. Time-averaged optical spectra of the DBR laser bar measured at temperatures of 25°C (black) and 45°C (red) and a pulse current of 0.74 kA.

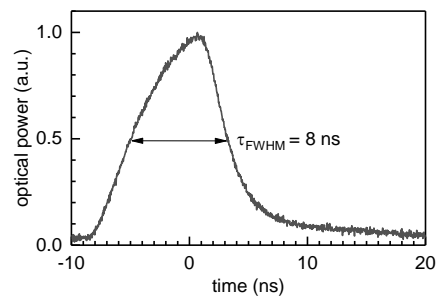


Fig. 4. Optical power versus time at a temperature of 25°C and a pulse current of 0.79 kA.

At the conference, we will present further details regarding the electrical driver and the electro-optical behavior of the bar and we will discuss reliability issues.

Acknowledgments

This work was supported by the Research Fab Germany under Ref. 16FMDQ2 and the German Federal Ministry of Education and Research (BMBF) grant 13N15566 as part of WiVoPro.

References

- [1] S. Victori, Proc. IEEE High Power Diode Lasers and Systems Conference, 3-6 (2019) DOI: 10.1109/HPD48113.2019.8938672
- [2] A. Klehr, A. Liero, H. Christopher, H. Wenzel, A. Maaßdorf, P. Della Casa, P., J. Fricke, A. Ginolas, A. Knigge, Semiconductor Science and Technology 35, 065016 (2020).
- [3] M. Müller, M. Philippens, G. Grönninger, H. König, J. Moosburger, G. Herrmann, M. Reufer, J. Luft, M. Stoiber, D. Lorenzen, Proc. SPIE 6456, 64561B (2007).
- [4] M. Kankar, Z. Chen, W. Dong, X. Guan, S. Zhang, S. Elim, L. Bao, M. Grimshaw, M. DeVito, J. Photon. Energy 7(1), 016003 (2017).
- [5] Y. Higa, M. Yoshida, N. Nishiyama, Y. Miyamoto, N. Kagi, Proc. ISLC 237-238 (2018).
- [6] Y. Zhao, U. Wang, A. Demir, G. Yang, S. Ma, B. Xu, C. Sun, B. Li, B. Qiu, IEEE Photonics Journal 13(3), 1-8 (2021).
- [7] S. O. Slipchenko, A. A. Podoskin, D. A. Veselov, V. A. Strelets, N. A. Rudova, N. A. Pikhtin, T. A. Bagaev, M. A. Ladugin, A. A. Marmalyuk and P. S. Kop'ev, IEEE Photonics Technology Letters 34, 35-38 (2022)
- [8] H. Wenzel, A. Maaßdorf, C. Zink, D. Martin, M. Weyers, A. Knigge, Electronics Letters 57, 445-447 (2021).
- [9] H. Wenzel, J. Fricke, A. Maaßdorf, N. Ammouri, C. Zink, D. Martin, A. Knigge, Electronics Letter 58, 121-123 (2022)
- [10] J. Fricke, H. Wenzel, O. Brox, P. Crump, B. Sumpf, K. Paschke, K., M. Mattala, G. Erbert, A. Knigge, G. Tränkle, Proc. SPIE 11301, 113011H (2020).